Saysunee Jumrat, Teerasak Punvichai, Wichuta Sae-jie, Seppo Karrila and Yutthapong Pianroj*

Simple microwave pyrolysis kinetics of lignocellulosic biomass (oil palm shell) with activated carbon and palm oil fuel ash catalysts

https://doi.org/10.1515/ijcre-2021-0231
Received September 8, 2021; accepted November 26, 2021; published online December 10, 2021

Abstract: The important parameters characterizing microwave pyrolysis kinetics, namely the activation energy (E_a) and the rate constant pre-exponential factor (A), were investigated for oil palm shell mixed with activated carbon and palm oil fuel ash as microwave absorbers, using simple lab-scale equipment. These parameters were estimated for the Kissinger model. The estimates for E_a ranged within 31.55–58.04 kJ mol^{-1} and for A within 6.40E0–6.84E+1 s^{-1}, in good agreement with prior studies that employed standard techniques: Thermogravimetric Analysis (TGA) and Differential Scanning Calorimetry (DSC). The E_a and A were used with the Arrhenius reaction rate equation, solved by the 4th order Runge-Kutta method. The statistical parameters coefficient of determination (R^2) and root mean square error (*RMSE*) were used to verify the good fit of simulation to the experimental results. The best fit had R^2 = 0.900 and *RMSE* = 4.438, respectively, for MW pyrolysis at power 440 W for OPS with AC as MW absorber.

***Corresponding author: Yutthapong Pianroj**, Faculty of Science and Industrial Technology, Prince of Songkla University Suratthani Campus, Muang, Surat-Thani, 84000, Thailand; and High-Value Integrated Oleochemical Research Center, Prince of Songkla University Suratthani Campus, Muang, Surat-Thani, 84000, Thailand, E-mail: yutthapong.p@psu.ac.th.
https://orcid.org/0000-0002-4500-1045
Saysunee Jumrat, Faculty of Science and Industrial Technology, Prince of Songkla University Suratthani Campus, Muang, Surat-Thani, 84000, Thailand; and High-Value Integrated Oleochemical Research Center, Prince of Songkla University Suratthani Campus, Muang, Surat-Thani, 84000, Thailand
Teerasak Punvichai, High-Value Integrated Oleochemical Research Center, Prince of Songkla University Suratthani Campus, Muang, Surat-Thani, 84000, Thailand; and Faculty of Innovation Agriculture and Fisheries Establishment Project, Prince of Songkla University Suratthani Campus, Muang Surat-Thani, 84000, Thailand
Wichuta Sae-jie and Seppo Karrila, Faculty of Science and Industrial Technology, Prince of Songkla University Suratthani Campus, Muang, Surat-Thani, 84000, Thailand

Keywords: microwave pyrolysis; oil palm fuel ash; oil palm shell; pyrolysis kinetics.

1 Introduction

Thailand is a developing county, and its economy is based on agricultural products and agro-industry. Therefore, biomass residues from these activities are abundant and low-cost in every part of Thailand. In the southern part of Thailand the main agricultural product is oil palm, and the value chain from this product involves crude palm oil mills and palm oil refineries. The crude palm oil mills use as their raw material fresh fruit bunches of oil palm to extract the crude palm oil, and the by-products from this processing are lignocellulosic biomass: empty fruit bunches, oil palm shell (OPS), and oil palm fiber (OPF), among others. Normally, both OPS and OPF residues are used as fuel burned in the factory boiler; and this again leaves residue from the combustion, namely palm oil fuel ash (POFA). The total annual solid waste from the crude palm oil mill industry in Thailand is estimated at around 2.1 million tons (Chavalparit et al. 2006). Therefore, value-added utilization of oil palm by-products or wastes has been considered in several studies, as shown in the good review by Foo and Hameed (2009b). The concepts addressed in studies include generating energy from oil palm waste, in the forms of palm leaves, palm fronds, palm trunks, empty fruit bunches, etc. (Chuah et al. 2006). The POFA was used as a microwave (MW) absorber to absorb MW energy to heat for MW pyrolysis, in a study by Chuayjumnong et al. (2020). Foo and Hameed (2009a) and Haydar and Aziz (2009) used POFA as a novel adsorbent, tested among a wide range of treatment technologies including precipitation, coagulation-flocculation, sedimentation, flotation, adsorption, and ion exchange. During the last 20 years, many studies (Sata, Jaturapitakkul, and Kiattikomol 2007; Tangchirapat et al. 2007) have assessed the utilization of oil palm ash as a supplementary cementitious material and a viable pozzolanic material for producing high-strength concrete. Yin et al. (2008) tested

POFA as sludge chemical binder for stabilizing pH, reducing mobility of contaminants, and improving precipitation, encapsulation, chemisorption, and ion exchange processes.

To utilize biomass or to add value to it, the chemical approach by pyrolysis is based on thermochemical conversion in the absence of oxygen, to produce target products such as biochar, bio-oil, and syngas. Microwaves (MW) have been used as an alternative heat source to pyrolyze various lignocellulosic biomass feedstocks, and the main advantages of MW are volumetric heating of the sample, rapid, selective, precise, and controlled heating (dependent on the material properties), low thermal inertia, and fast response (Chen et al. 2016; Huang, Chiueh, and Lo 2016; Pianroj et al. 2016; Reddy et al. 2019; Yerrayya et al. 2018; Zhang et al. 2017). Moreover, the ability of microwave heating to process a wide variety of biomasses is a tremendous benefit when it comes to processing feedstock with a high moisture content. A characteristic feature of this technique is the ability to manipulate the heating rate of a sample without increasing the input power, through the use of microwave absorbers (MWAbs), also known as susceptors (Francis Prashanth, Midhun Kumar, and Vinu 2020).

Evaluation and understanding of the pyrolysis kinetics and mechanisms of thermochemical biomass conversion are essential for the design, optimization, and scale-up of industrial thermochemical biomass reactors (Gogoi et al. 2018; Wang et al. 2018). Normally, the most widely used reliable characterization techniques, Thermogravimetric Analysis (TGA) and Differential Scanning Calorimetry (DSC), are used to evaluate the pyrolysis kinetics and other reaction parameters of an energetic biomass (Cai et al. 2018; Jain, Mehra, and Ranade 2016; Kristanto, Azis, and Purwono 2021; Müsellim et al. 2018; Özsin and Pütün 2019; Rasool and Kumar 2020; Williams and Nugranad 2000). However, this current study aimed to investigate and identify the pyrolysis kinetics, specifically the parameters activation energy (E_a) and rate constant pre-exponential factor or frequency factor (A), of MW pyrolysis with different types of MWAb by using simple equipment. These two parameters were identified in the Kissinger model and the estimates were compared with previous literature data from using the standard equipment: TGA and DSC. Finally, these important parameters were fitted by solving the general reaction rate with temperature dependence given by the Arrhenius equation, and the numerical solution method was the 4th order Runge-Kutta method. The parameter estimation from least-squares fits between experimental and simulation data iteratively maximized the coefficient of determination (R^2) and minimized the root mean square error (*RMSE*).

2 Materials and methods

2.1 Materials

In this experiment, the oil palm shell (OPS) lignocellulosic biomass, and the palm oil fuel ash (POFA) for use as a microwave absorber (MWAb), were obtained from palm oil mills of the Green Glory co., Ltd., at Tha-Chang, in Surat-Thani province of Thailand. A commercial grade activated carbon (AC) for water treatment, based on coconut shells, was used as an alternative catalyst. The OPS was ground to 1.18–2.00 mm particle size range, and both OPS and POFA were dried in an oven at 105 °C to reduce the moisture content to approximately 8.50 %wb, and then they were kept in zip-lock plastic bags to maintain the moisture content. The feedstocks were subjected to proximate analysis (ASTM D7582 by Thermogravimetric Analyzer, TGA7, PerkinElmer, USA) and ultimate analysis (CHNS-O Analyzer, CE Instrument Flash EA1112 Series, Thermo Quest, Italy), and the composition of POFA was characterized by X-ray Fluorescence Spectrometry (XRF spectrometer, Zetium, PANalytical, Netherlands). It is noted that all these analyses were run by the Office of Scientific Instruments and Testing (OSIT), Prince of Songkla University, Hat-Yai Campus.

2.2 Experimental set-up

These experiments were carried out in a domestic multimode microwave oven with maximum power output rated as 800 W at 2.45 GHz microwave frequency. The microwave oven was modified by removing the base of the turntable, and a hole with 25 mm diameter was drilled on top of the oven. The electrical system for ON–OFF control of the microwave oven was modified, so that the power cord was coupled with a pair of clamps to an electronic switch. A stirrer rotated by a geared motor was installed so that it was turned on or off along with the rest of the system. The stirrer had a metallic propeller and motor driving it at 50 rpm to disturb (homogenize) the microwave electric field: its purpose was to make the heating inside the cavity uniform across a sample. For electrical grounding copper ingots were buried in the ground and the microwave as well as thermocouples were grounded, to reduce measurement noise while the microwave is on.

The 250 mL reactor was made of quartz, flask-shaped, with narrow mouth and internal diameter of 23 mm, external diameter of 32 mm, and height of 140 mm. Teflon corks were made for use as lid, to height 40 mm and diameter 22 mm, with three holes of 7 mm in diameter drilled in this stopper so that glass tubes could be inserted. Each hole had a different function. Hole 1, for a bent glass tube was intended for inflow of N_2 flushing. The bent glass tube was coupled by a hose to a rotameter with a valve, for control of N_2 flowrate. Hole 2, for inserting a straight glass tube was intended for the type-K thermocouple probe: a metal sheet is needed around the glass tube to reduce interference from the microwaves. The third hole was for a long glass tube to vent out the pyrolysis product gases to the condensation system. A ceramic cup was used as base to support the quartz reactor, with an insulation layer between these to prevent rattling, reduce friction, and shield against burns.

The temperature feedback control system had the type-K thermocouple provide an analog signal to the temperature controller SHIMAX™ model MAC3D-MSF-EN-NRN. This was the command unit controlling the solid-state relay (SSR). This SSR functioned as an ON–OFF switch of the electric microwave power supply. The

temperature controller also communicated with a personal computer (PC) by RS485 to RS232 for collecting temperature data. The thermocouple was inserted into the sample from the top of the reactor. The method of operation was to set the desired temperature value, set the maximum and minimum temperatures, and during a run the real-time temperature was displayed and all data were logged by the Shimax software. Figure 1 shows the temperature controller, and RS485 and RS232 ports.

Before the pyrolysis run, N_2 flushing of the reactor was done for 2 min to ensure that the sample was in inert atmosphere, because pyrolysis requires oxygen-free heating. This flushing removed oxygen from the system and during a run moved pyrolysis products to the condensation section of the setup. N_2 is colorless, odorless, non-toxic, and non-flammable gas and its flow rate were set at four LPM. The inert gas could also play an important role in ensuring safety during the experiment, as it helps avoid explosion or other risks potentially caused by accumulation of volatile compounds. During the runs, care was taken to prevent any product gas leaks from the system, as it had elevated pressure and a high temperature. After the pyrolysis was complete, N_2 flushing of the system was continued for another 2 min to remove heat from the system. Then liquid products were collected from both parts of the condensing system.

The optimum conditions from the previous work of Chuayjumnong et al. (2020) were determined to maximize the liquid product with each type of MWAb, and were adopted in this study of pyrolysis kinetics. In the experimental runs the time profiles of weights were determined. Before the experiment, a glass tube was placed in a hole at the bottom of the microwave oven so that the top of the glass tube would support the weight of the sample, and the bottom end of that glass tube was on a weighing scale that sent its reading to the computer during a run. In this experiment, insulation between glass tubes and quartz reactor was used. After that, the runs used three alternative microwave power levels of 440, 616, and 800 W, for a pyrolysis time of 20 min. Throughout the experiments, the N_2 flow rate was set at four LPM. Figure 1 shows a schematic diagram of the system for the study of microwave pyrolysis kinetics. After the experiment was completed, the data were used to estimate the activation energy in the microwave pyrolysis of OPS with each type of MWAb, by using the Arrhenius equation and the Kissinger method.

2.3 Theory background on reaction kinetics

In this study, the reaction kinetics analysis of oil palm shell (OPS) microwave (MW) pyrolysis applied the Kissinger method (Huang et al. 2016; Kissinger 1957). Mostly the kinetics of a reaction of the type "*solid* → *solid* + *gas*" can be described by Eq. (1).

$$\frac{dx}{dt} = Ae^{-E_a/RT}(1-x)^n \tag{1}$$

$$x = \frac{m_0 - m_t}{m_0 - m_f} \tag{2}$$

where dx/dt is the rate of change of mass fraction, m_0 and m_f are the initial and final masses of the sample, respectively, m_t is sample mass at time t, and n is the empirical order of the reaction. This includes the Arrhenius equation for the rate constant k as described in Eq. (3).

$$k = A\exp\left(\frac{-E_a}{RT}\right) \tag{3}$$

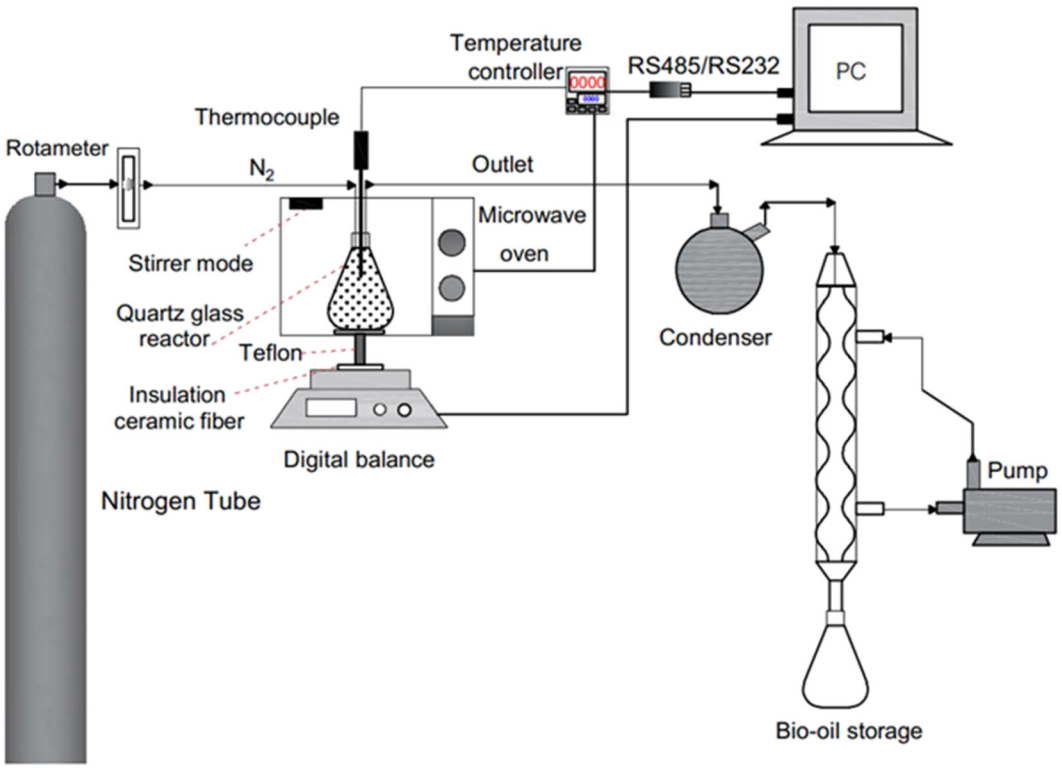

Figure 1: Schematic diagram of the experimental microwave pyrolysis system for studying pyrolysis kinetics.

where A is the rate constant pre-exponential factor or frequency factor, E_a is the activation energy (kJ mol^{-1}), R is the universal gas constant (8.314 J mol^{-1} K^{-1}), and T is the absolute temperature (K). The temperature rises during the reaction, so the reaction rate dx/dt will increase to its maximum, then return to zero as the reactant is exhausted. Assuming that the temperature rises at a constant heating rate β and differentiating Eq. (1), the Kissinger model is obtained in Eq. (4).

$$\ln\left(\frac{\beta}{RT_{max}^2}\right) = -\frac{E_a}{RT_{max}} + \ln\left(\frac{A}{E_a}\right) \quad (4)$$

in which T_{max} is the maximum temperature. From Eq. (4), the plot of $\ln(\beta/RT_{max}^2)$ versus $1/T_{max}$ should give a straight line. The slope and intercept of the fitted line can be used to estimate the activation energy and pre-exponential factor for MW pyrolysis.

3 Results and discussion

3.1 Compositions of biomass feedstocks and microwave absorbers

By its physical appearance, the OPS was brown particles, solid, irregularly flat, curved and concave on the surface, relatively smooth, with some residual fibers, with edges of surfaces and cracks sharp, and the heating value was quite high. The sharpness and appearance of the cracks depend on the cracking of the palm fruit. AC was made from coconut shell and was commercial grade porous carbon. By physical characteristics, the AC was granular, black, very porous, and brittle. POFA was formed by combustion of OPS and oil palm fiber from the palm oil extraction process in a boiler, and the ash appeared heavy. By physical characteristics, the POFA was powdery, lightweight, easily dusting, and dark black. In the presence of moisture, it will cake or clump, the particles are of irregular sizes, and there is a small amount of oil palm fiber. Lower temperature firing produces black to dark gray POFA due to the high content of unburned carbon, known as ground POFA. The higher the firing temperature the less there is unburned carbon, thus giving it a lighter color and better appearance; this is called unground POFA. In specific gravity ground POFA is heavier, while the particle size of unground POFA is larger than in ground POFA. Figure 2 shows the appearances of OPS, POFA, and AC in this current study.

The results of the OPS analysis in Table 1 (Pianroj et al. 2016) are for the Thaksin Palm Oil Mill in the factory area in Suratthani province, as well as the OPS used for testing. Due to the physical nature and hardness of OPS, it can be considered a natural lignocellulosic material (Asadullah et al. 2013). The results show that the compositions of AC and POFA specified in Table 1 (given in wt% by dry weight) had moisture contents approximately 8.88 ± 0.0 and

Figure 2: Appearances of OPS, POFA, AC.

Table 1: Proximate and ultimate analyses of OPS, AC, and POFA.

Parameter	OPS[a]	AC	POFA
Moisture content (wt%)	11.39 ± 0.00	8.88 ± 0.04	5.23 ± 0.27
Volatile matter (wt%)	65.76 ± 0.00	8.22 ± 0.27	6.53 ± 0.29
Fixed carbon (wt%)	19.73 ± 0.00	71.50 ± 0.26	11.76 ± 1.32
Ash (wt%)	3.117 ± 0.00	2.40 ± 0.04	78.48 ± 1.87
Carbon (C) (wt%)	45.65 ± 0.26	75.99 ± 0.18	17.42 ± 0.23
Hydrogen (H) (wt%)	5.49 ± 0.06	1.88 ± 0.03	0.41 ± 0.01
Nitrogen (N) (wt%)	0.32 ± 0.01	0.13 ± 0.01	0.16 ± 0.01
Sulfur (S) (wt%)	Not detected	<0.01	0.30 ± 0.01
Oxygen (O) (wt%)	36.59 ± 0.36	14.60 ± 0.12	4.39 ± 0.02
Net heating value (N.H.V) (kcal kg^{-1})	29,522.48 ± 0.00[b]	6155.11 ± 10.30	1367.63 ± 16.82

[a]According to Pianroj et al. (2016), [b]According to Onochie et al. (2015).

5.23 ± 0.27 wt%, respectively, and the volatile carbon content and ash (dry) were approximately 71.50 ± 0.26 and 11.76 ± 1.32 wt%, respectively. The amount of carbon combustible of AC was 75.99 ± 0.18, while POFA had only 17.42 ± 0.23 wt%. The amounts of hydrogen, oxygen, and nitrogen in AC were approximately 1.88 ± 0.03, 14.60 ± 0.12, and 0.13 ± 0.01 wt%, respectively. The amounts of hydrogen, oxygen, and nitrogen in POFA were approximately 0.41 ± 0.01, 4.39 ± 0.02, and 0.16 ± 0.01 wt%, respectively. It can be observed that these materials have otherwise similar compositions, but the carbon contents are very different. On the other hand, the POFA ash content was greater than that of AC. This may be because POFA had been burned at a high temperature (800–1000 °C) (Awang and Al-Mulli 2018), resulting in less carbon remaining than in AC. Also, this analysis is related to the dielectric properties. Also, the net heating value was measured in a Bomb Calorimeter. The chemical components of POFA as characterized by XRF technique are shown in Table 2.

3.2 Pyrolysis kinetics and temperature profiles

In an earlier study, Chuayjumnong et al. (2020) had activated carbon (AC) and palm oil fuel ash (POFA) as microwave absorbers (MWAbs) in the microwave-assisted pyrolysis of oil palm shell (OPS). The results showed that the highest bio-oil yield was obtained at 500 °C with OPS:AC and OPS:POFA blend ratios at 70:30; and moreover, the AC and POFA did not significantly differ in bio-oil yields (Chuayjumnong et al. 2020). Therefore in this study, the microwave pyrolysis kinetics and temperature profiles of OPS:AC and OPS:POFA blends at 70:30 ratio were studied at MW power levels of 440, 616, and 800 W. All results from pyrolysis run kinetics and time profiles of temperature are shown in Figure 3.

In the left panels of Figure 3, i.e. Figure 3a and c, the pyrolysis kinetics and temperature profile are shown for OPS:AC, while in the right panels (Figure 3b and d), similar profiles are shown for OPS:POFA, and each panel has separate curves for the microwave levels 440, 616, and 800 W. There are no surprises in these results as increasing MW power increased weight loss and temperature with steeper slopes in all graphs. These data are for real experimental runs, and the first period around 0–5 min dominates all changes. The volatiles were vaporized in this period, so that the weight decreased sharply, along with a rapid increase in temperature. Then both weight and temperature remained practically steady from the 6th min to the end of the run. No volatiles were vaporized in this steady period. However, the pyrolysis kinetics and thermal behaviors can be compared between the two MWAbs at the alternative MW power levels tested. In the case of using AC as MWAb (Figure 3a and 3c), it was found that the weight decreased to 50, 45, and 43%, and the maximum temperatures were 799, 900, and 951 °C, as the MW power increased from 440 to 616, and to 800 W. In the case of POFA as MWAb (Figure 3b and d), the weight losses were 37, 36, and 35%, and the maximum temperatures were 909, 980, and 1040 °C, in the same order. It is important to assess from these experiments whether the different pyrolysis conditions affected the distribution of products, which has earlier been reported by Chuayjumnong et al. (2020).

Table 2: The chemical components of POFA as analyzed by X-ray fluorescence spectrometry (XRF).

No.	Chemical components	%Concentration
1	Silicon dioxide (SiO_2)	51.20
2	Calcium oxide (CaO)	8.05
3	Potassium oxide (K_2O)	7.20
4	Phosphorus pentoxide (P_2O_5)	4.14
5	Magnesium oxide (MgO)	3.29
6	Aluminum oxide (Al_2O_3)	2.10
7	Sulfur trioxide (SO_3)	1.48
8	Ferric oxide (Fe_2O_3)	1.45
9	Other components[a]	1.09

[a]Other components; Chloride (Cl), Titanium dioxide (TiO_2), Manganese oxide (MnO_2), Sodium oxide (Na_2O), Copper oxide (CuO), Strontium oxide (SrO), Rubidium oxide (Rb_2O), Chromic oxide (Cr_2O_3), Zirconium dioxide (ZrO_2), and Zinc oxide (ZnO).

3.3 Reaction kinetics

To express the reaction kinetics of oil palm shell (OPS) microwave (MW) pyrolysis, some parameters of the Kissinger model in Eq. (4) can be obtained from the experiments, like the maximum temperature and the heating rate. First, the maximum temperatures at each MW power level (440, 616, and 800 W) with activated carbon (AC) as microwave absorber (MWAb) were 799, 900, and 951 °C, respectively, while with palm oil fuel ash (POFA) these were 909, 980, and 1040 °C. All the data were plotted versus the MW power level, as shown in Figure 4, and the data were fit with least squares in the linearized equation form by using Microsoft Excel, and the equations and their coefficients of determination (R^2) were recorded.

Next, the heating rate is important as it affects the quantity and the composition of volatile substances in biomass during pyrolysis. The heating rates for each MW

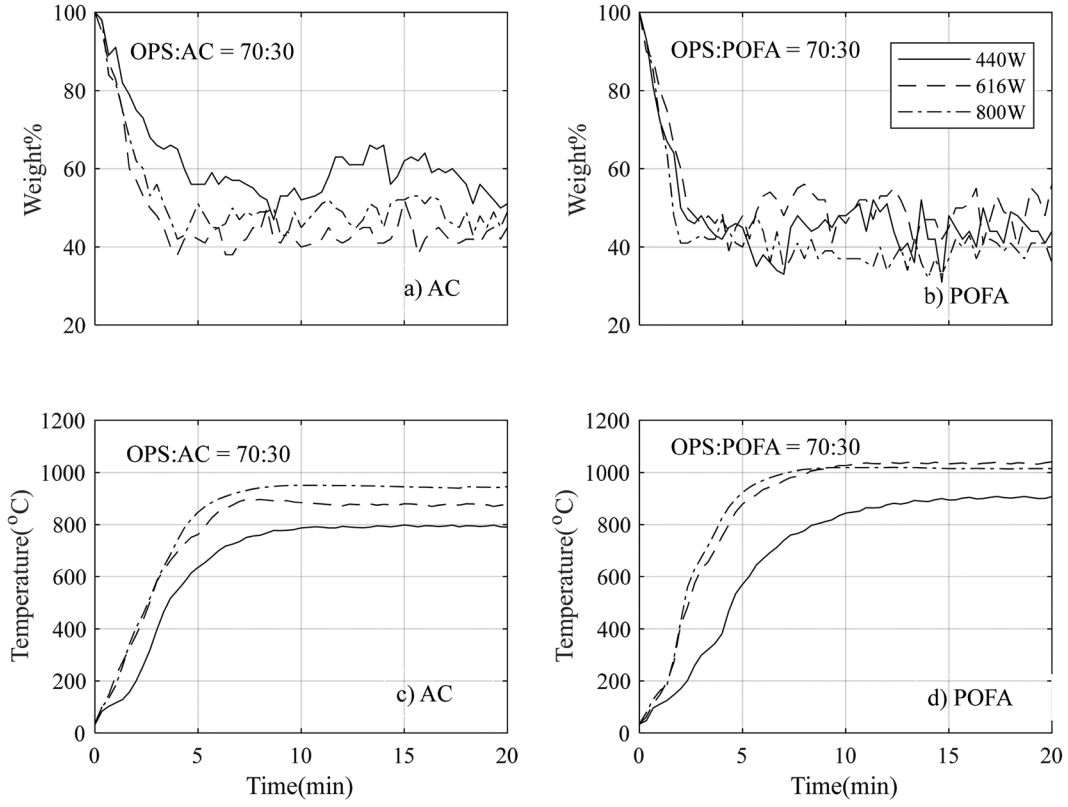

Figure 3: Time profiles of weight and temperature in MW pyrolysis of OPS at various MW power levels, with AC or POFA as MW absorber.

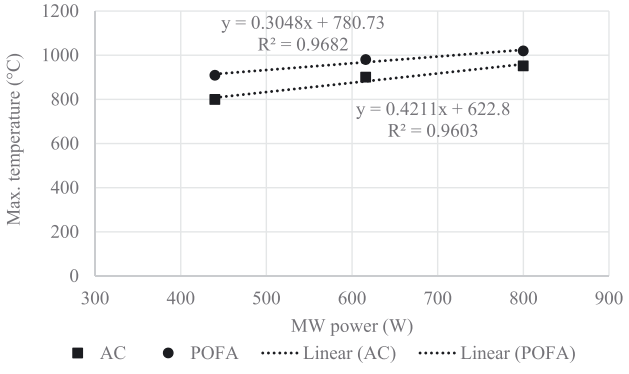

Figure 4: Plot of the maximum temperatures at different MW power levels using AC or POFA as MWAb.

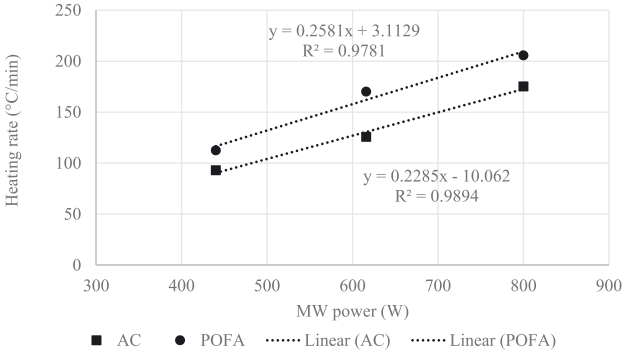

Figure 5: Plot of heating rates with AC or POFA as MWAb versus MW power.

power level with AC or POFA are the slopes ($\Delta T/\Delta t$) in Figure 3c and d, and were estimated for the first period of 0–5 min in each run. It was found that the heating rates with AC as MWAb were 93.00, 125.78, and 175.15 °C min^{-1} for MW power levels 440, 616, and 800 W, respectively, and the corresponding heating rates with POFA as MWAb were 112.57, 170.12, and 205.66 °C min^{-1}, respectively. The heating rates were fit with linear least squares in Microsoft Excel as shown in Figure 5 for both AC and POFA.

Using the fits for interpolation by Eq. (4), the results in Tables 2 and 3 were obtained for AC or POFA as MWAb, respectively.

The Arrhenius reaction rate constant (k) has been verified empirically to give the correct temperature behavior for most reaction rate constants within experimental accuracy over fairly large temperature ranges. Additionally, the activation energy can be thought of in two conceptual scenarios (Fogler 2020). Firstly, in the collision theory, kinetic energy is transferred through atom

Table 3: Interpolation of MW pyrolysis performance for OPS with AC as MWAb.

MW power (W)	Heating rate (°C min^{-1})	T_{max} (°C)	T_{max} (K)	$1/T_{max}$	ln (β/RT^2_{max})
450	92.76	812.75	1085.75	0.00092	−11.57
500	104.19	833.86	1106.86	0.00090	−11.49
550	115.61	854.96	1127.96	0.00089	−11.42
600	127.04	876.07	1149.07	0.00087	−11.37
650	138.46	897.17	1170.17	0.00085	−11.32
700	149.89	918.28	1191.28	0.00084	−11.27
750	161.31	939.38	1212.38	0.00082	−11.24
800	172.74	972.74	1233.49	0.00081	−11.20

and molecule collisions to internal energy for stretching and bending bonds. Secondly, activation energy acts as a barrier to energy transfer from kinetic energy to potential energy between reacting atoms and molecules, and it needs to be overcome. To investigate MW pyrolysis kinetics of OPS with AC or POFA as MWAb, the Arrhenius reaction rate constant (k) was plotted as a function of pyrolysis temperature, with results shown in Figure 7. The AC gave larger values than POFA in the range 400–800 °C, while in the temperature range 800–1400 °C the POFA caught up with AC and passed by it, given final temperatures higher than AC. These trends and results were found also earlier by Chuayjumnong et al. (2020). This indicates that OPS with AC as MWAb has a lower activation energy than with POFA as MWAb, so that the barrier to energy transfer from kinetic to potential energy between molecules is easier to overcome.

Finally, Figure 6a and b) show the straight line fits in plots of ln (β/RT^2_{max}) versus $1/T_{max}$ for AC and POFA, based on data in Tables 3 and 4, respectively. The slope of a straight line shows the activation energy (E_a) and the intercept gives the pre-exponential factor (A). The averages of E_a and A estimates in the range of MW power tested (400–800 W) for OPS with AC were 31.55 kJ mol^{-1} and 6.40 (s^{-1}); while in the case of POFA as MWAb the estimates of E_a and A were 58.04 kJ mol^{-1} and 68.40 (s^{-1}), respectively. These results agree with prior studies, as shown in Table 5. However, it is very difficult to identify the exact values or the causes of variations in these parameters. Salema, Ting, and Shang (2019) and the good review article by

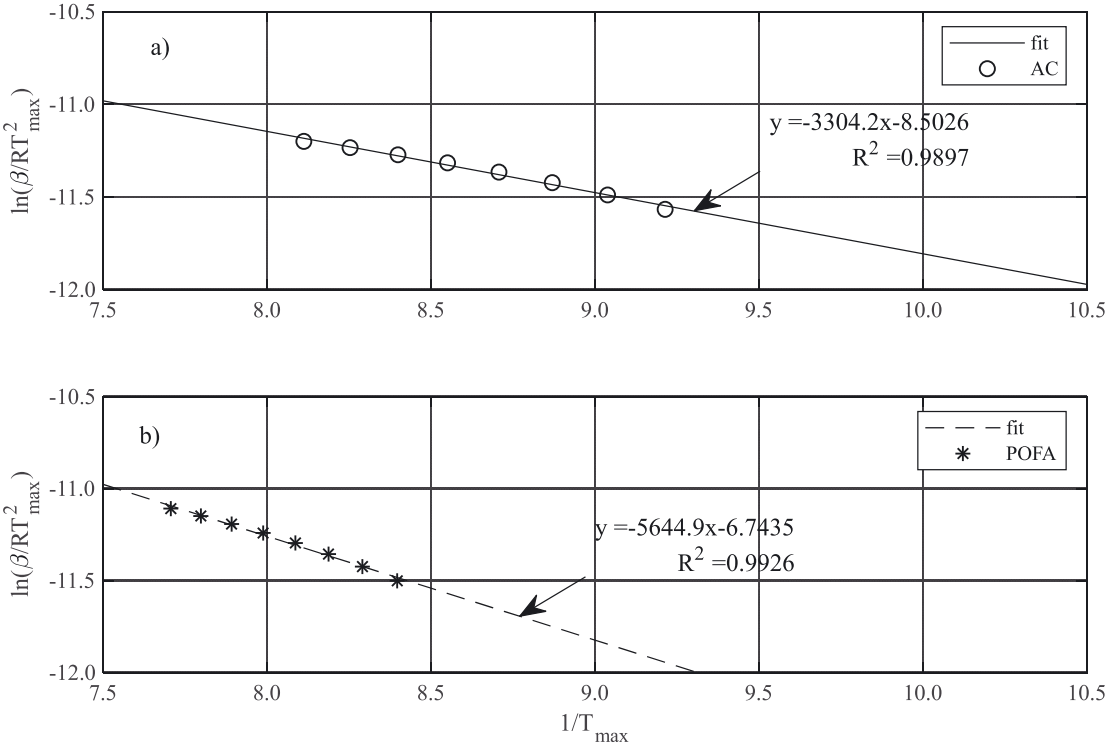

Figure 6: Plots of ln (β/RT^2_{max}) versus $1/T_{max}$ for OPS with (a) AC, and (b) with POFA as MWA.

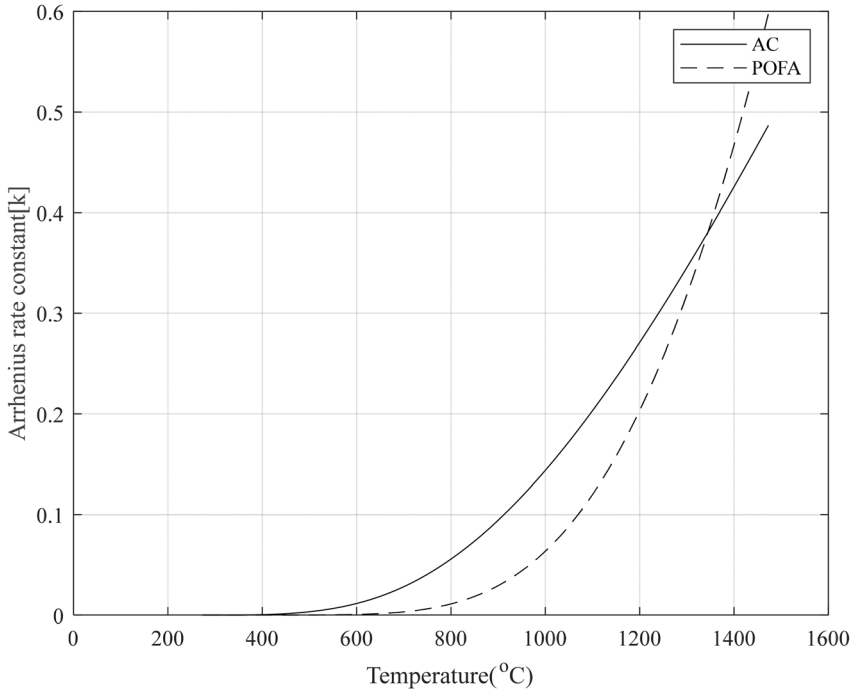

Figure 7: The Arrhenius reaction rate constant plotted versus the MW pyrolysis reaction temperature for OPS with AC or with POFA as MWAb.

Table 4: Interpolation of MW pyrolysis performance for OPS with POFA as MWAb.

Power (W)	Heating rate (°C min^{-1})	T_{max} (°C)	T_{max} (K)	$1/T_{max}$	ln (β/RT^2_{max})
450	119.26	917.89	1190.89	0.00084	−11.50
500	132.16	933.13	1206.13	0.00083	−11.42
550	145.07	948.37	1221.37	0.00082	−11.36
600	157.97	963.61	1236.61	0.00081	−11.30
650	170.88	978.85	1251.85	0.00080	−11.24
700	183.78	994.09	1267.09	0.00079	−11.19
750	196.69	1009.33	1282.33	0.00078	−11.15
800	209.59	1024.57	1297.57	0.00077	−11.11

Table 5: Comparision of E_a and A parameters for OPS with prior literature data.

Reference	E_a (kJ mol^{-1})	A (1/s)
Present work	31.55–58.04	6.40E0–6.84E+1
Lee et al. (2017)	84.0–445.05	–
Mohd Din, Hameed, and Ahmad (2005)	5.7–65.3	1.53E−4–877E+1
Salema, Ting, and Shang (2019)	40.49–109.11	4.51E−1–6.36E+7

White, Catallo, and Legendre (2011) mention that these parameters are affected by reaction conditions, including temperature, heating rate, residence time, particle size, pressure, gaseous atmosphere, and the presence of inorganic minerals in the biomass. Moreover, Rodilla, Contreras, and Bahillo (2018) found that variations in these results could be caused by reaction mechanisms that are too complex to predict, while other causes of variations include accelerated heating, high volatile matter content, catalytic effects (Mallick et al. 2018), biomass blend ratio, and coal-biomass blend proportions (Jayaraman, Kok, and Gokalp 2017). Huang et al. (2016) found that increasing MW power level increased E_a and A, which means that a higher power level provides more weight loss. It can be seen that energy is needed to decompose the thermally-resistant part of biomass.

Therefore, this study has demonstrated that MW pyrolysis kinetics can be identified by simple tools, such as a slightly modified microwave oven, to characterize feedstock blends. Also, the heating rate, the maximum temperature, the weight loss, and the activation energy were obtained from the kinetic analysis of OPS microwave pyrolysis.

3.4 Numerical simulation of pyrolysis kinetics

The solid-state pyrolysis kinetics of biomass complied with the general reaction rate equation Eq. (1). The dynamic situation is represented by a 1st order ordinary differential equation (ODE). To solve this ODE, a high accuracy numerical method, namely the 4th order Runge-Kutta (RK), was applied to solving the reaction rate equation with the empirical order set to 1 (n = 1). In order to optimize the

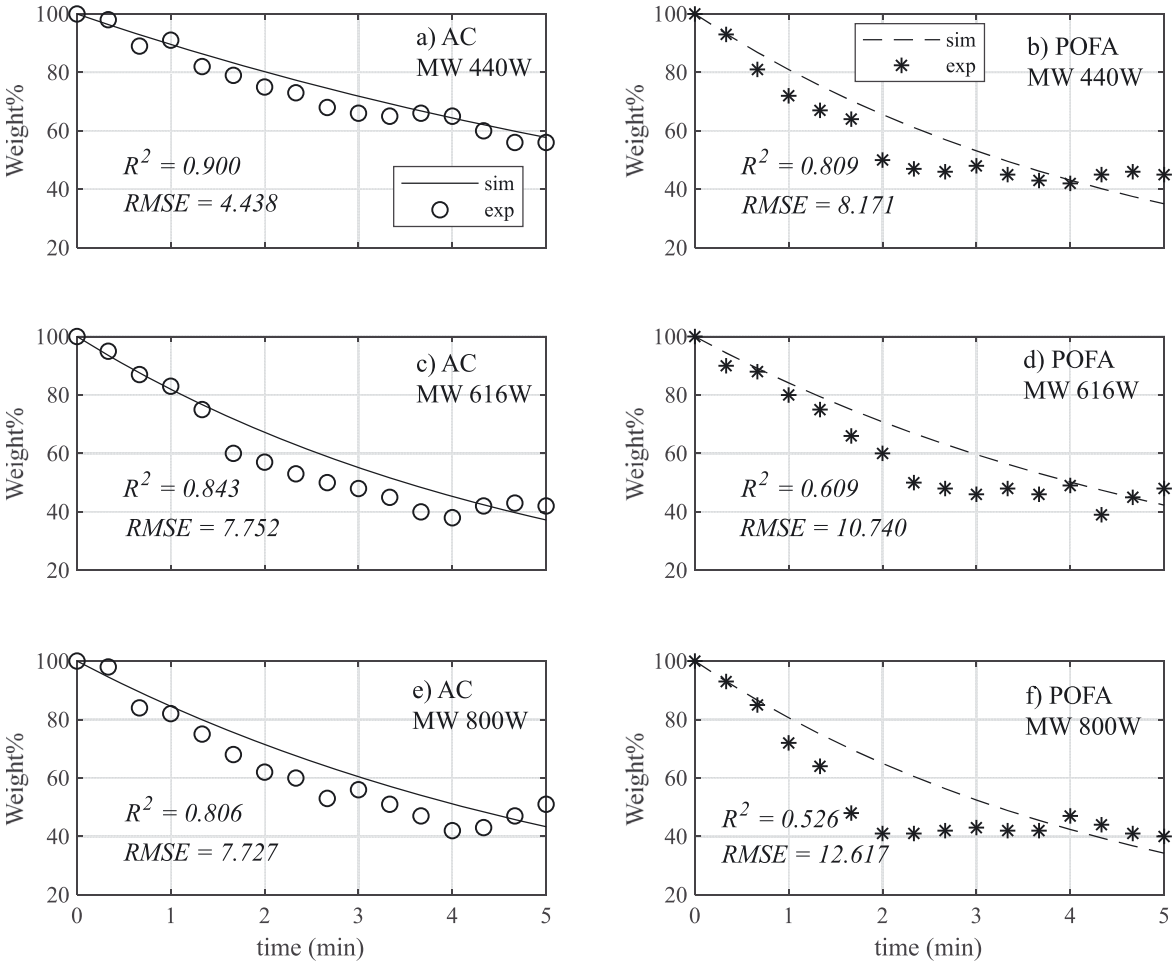

Figure 8: The simulations and experimental results on sample weight plotted as functions of pyrolysis time for OPS with AC of POFA as MWAb, at each MW power level.

simulation parameters used by the RK method, to better agree with the experimental data for each microwave power level, iterations were applied to maximize the coefficient of determination (R^2) and to minimize the root mean square error (*RMSE*) defined in Eq. (5).

$$RMSE = \sqrt{\frac{1}{N}\sum_{i=1}^{N}\left(X_{\mathrm{sim},i} - X_{\mathrm{exp},i}\right)^2} \tag{5}$$

where $X_{\mathrm{exp},i}$ and $X_{\mathrm{sim},i}$ refer to the experimental and simulated mass fractions remaining, respectively, and N is the number of data points. The scanned ranges of the kinetic parameters, activation energy (E_a) and the rate constant pre-exponential factor (A), came from Table 4 using initial T = 313 K. The optimal results matching simulations and experiments in the first period of 0–5 min of pyrolysis time for OPS with AC of POFA as MWAb at each MW power level are shown in Figure 8.

The cases with AC as MWAb are shown on the left in Figure 8, while those with POFA as MWAb are on the right side. The simulations of AC compared with the experiment results had R^2 in 0.806–0.900 and *RMSE* in 4.438–7.752, while these ranges with POFA were 0.526–0.809 and 8.171–12.617, respectively. The ranges of R^2 and *RMSE* with AC were narrower and better than those with POFA, because AC absorbed MW energy better, quickly converting it into heat in the initial period of pyrolysis, as evidenced in Figure 7. However, the measurements of sample weights were less than ideal, having fluctuations in the signals from the digital balance.

4 Conclusions

The Arrhenius type temperature dependence in reaction kinetics for the microwave (MW) pyrolysis of oil palm shell (OPS), with either activated carbon (AC) or palm oil fuel ash (POFA) as the microwave absorber (MWAb), was demonstrated with simple laboratory scale experiments.

The results show that the average of activation energy (E_a) and the rate constant pre-exponential factor (A) for MW pyrolysis (power 400–800 W) of OPS using AC or POFA as a MWAb were 31.55 kJ mol^{-1} and 6.40 (s^{-1}), or 58.04 kJ mol^{-1} and 68.40 (s^{-1}), respectively. The estimates agreed with previous studies, which have used standard methods, such as thermogravimetric analysis (TGA), differential thermal gravimetry (DTG), and differential scanning calorimetry (DSC). However, a disadvantage of the simple lab-scale setup was the fluctuating weight data, and this should be improved for more accurate and precise results.

Nomenclature

Symbols

E_a	Activation energy (kJ mol^{-1})
A	Rate constant pre-exponential factor or frequency factor (s^{-1})
R	Universal gas constant (8.314 J mol^{-1} K^{-1})
T	Temperature (K)
T_{max}	Maximum temperature (K)
n	The empirical order of the reaction (–)
x	Mass fraction (–)
m_0, m_f, and m_t	Sample masses: initial, final, and at time t (kg)
k	Rate constant of Arrhenius equation (–)
R^2	Coefficient of determination (–)
RMSE	Root mean square error (–)

Greek letters

β	Heating rate (°C min^{-1})

Subscripts

OPS	Oil palm shell
OPF	Oil palm fiber
POFA	Palm oil fuel ash
AC	Activated carbon
MW	Microwave
MWAb	Microwave absorber
TGA	Thermogravimetric analysis
DSC	Differential scanning calorimetry
DTG	Differential thermal gravimetry

Acknowledgements: Authors thank Miss Sunisa Chuayjumnong, who carried out the experimental runs.
Author contributions: All the authors have accepted responsibility for the entire content of this submitted manuscript and approved submission.
Research funding: This project is funded by National Research Council of Thailnad (NRCT) under contact number 131/2563, Prince of Songkla University, Suratthani Campus, and Research and Development Office (RDO), Prince of Songkla University Hat-Yai Campus under the Research Center of High-Value Integrated Oleochemical.
Conflict of interest statement: The authors declare no conflicts of interest regarding this article.

References

Asadullah, M., N. S. Ab Rasid, S. A. S. A. Kadir, and A. Azdarpour. 2013. "Production and Detailed Characterization of Bio-Oil from Fast Pyrolysis of Palm Kernel Shell." *Biomass and Bioenergy* 59 (12): 316–24.

Awang, H. B., and M. Z. Al-Mulli. 2018. *The Inclusion of Palm Oil Ash Biomass Waste in Concrete: A Literature Review*. London: IntechOpen.

Cai, J., D. Xu, Z. Dong, X. Yu, Y. Yang, S. W. Banks, and A. V. Bridgwater. 2018. "Processing Thermogravimetric Analysis Data for Isoconversional Kinetic Analysis of Lignocellulosic Biomass Pyrolysis: Case Study of Corn Stalk." *Renewable and Sustainable Energy Reviews* 82 (2): 2705–15.

Chavalparit, O., W. H. Rulkens, A. P. J. Mol, and S. Khaodhair. 2006. "Options For Environmental Sustainability of the Crude Palm Oil Industry in Thailand Through Enhancement of Industrial Ecosystems." *Environment, Development and Sustainability* 8 (2): 271–87.

Chen, P., Q. Xie, M. Addy, W. Zhou, Y. Liu, Y. Wang, Y. Cheng, K. Li, and R. Ruan. 2016. "Utilization of Municipal Solid and Liquid Wastes for Bioenergy and Bioproducts Production." *Bioresource Technology* 215 (9): 163–72.

Chuah, T. G., A. G. K. Wan Azlina, Y. Robiah, and R. Omar. 2006. "Biomass as the Renewable Energy Sources in Malaysia: An Overview." *International Journal of Green Energy* 3 (3): 323–46.

Chuayjumnong, S., S. Karrila, S. Jumrat, and Y. Pianroj. 2020. "Activated Carbon and Palm Oil Fuel Ash as Microwave Absorbers for Microwave-Assisted Pyrolysis of Oil Palm Shell Waste." *RSC Advances* 10 (8): 32058–68.

Fogler, H. S. 2020. *Elements of Chemical Reaction Engineering*, 5th ed. USA: Pearson Education, Inc.

Foo, K. Y., and B. H. Hameed. 2009a. "A Short Review of Activated Carbon Assisted Electrosorption Process: An Overview, Current Stage and Future Prospects." *Journal of Hazardous Materials* 170 (2–3): 552–9.

Foo, K. Y., and B. H. Hameed. 2009b. "Value-Added Utilization of Oil Palm Ash: A Superior Recycling of the Industrial Agricultural Waste." *Journal of Hazardous Materials* 172 (2): 523–31.

Francis Prashanth, P., M. Midhun Kumar, and R. Vinu. 2020. "Analytical and Microwave Pyrolysis of Empty Oil Palm Fruit Bunch: Kinetics and Product Characterization." *Bioresource Technology* 310 (9): 123394.

Gogoi, M., K. Konwar, N. Bhuyan, R. C. Borah, A. C. Kalita, H. P. Nath, and N. Saikia. 2018. "Assessments of Pyrolysis Kinetics and Mechanisms of Biomass Residues Using Thermogravimetry." *Bioresource Technology Reports* 4 (12): 40–9.

Haydar, S., and J. A. Aziz. 2009. "Coagulation–flocculation Studies of Tannery Wastewater Using Combination of Alum with Cationic and Anionic Polymers." *Journal of Hazardous Materials* 168 (2): 1035–40.

Huang, Y.-F., P.-T. Chiueh, W.-H. Kuan, and S.-L. Lo. 2016. "Microwave Pyrolysis of Lignocellulosic Biomass: Heating Performance and Reaction Kinetics." *Energy* 100 (4): 137–44.

Huang, Y.-F., P.-T. Chiueh, and S.-L. Lo. 2016. "A Review on Microwave Pyrolysis of Lignocellulosic Biomass." *Sustainable Environment Research* 26 (3): 103–9.

Jain, A. A., A. Mehra, and V. V. Ranade. 2016. "Processing of TGA Data: Analysis of Isoconversional and Model Fitting Methods." *Fuel* 165 (2): 490–8.

Jayaraman, K., M. V. Kok, and I. Gokalp. 2017. "Thermogravimetric and Mass Spectrometric (TG-MS) Analysis and Kinetics of Coal-Biomass Blends." *Renewable Energy* 101 (2): 293–300.

Kissinger, H. E. 1957. "Reaction Kinetics in Differential Thermal Analysis." *Analytical Chemistry* 29 (11): 1702–6.

Kristanto, J., M. M. Azis, and S. Purwono. 2021. "Multi-distribution Activation Energy Model on Slow Pyrolysis of Cellulose and Lignin in TGA/DSC." *Heliyon* 7 (7): e07669.

Lee, X. J., L. Y. Lee, S. Gan, S. Thangalazhy-Gopakumar, and H. K. Ng. 2017. "Biochar Potential Evaluation of Palm Oil Wastes Through Slow Pyrolysis: Thermochemical Characterization and Pyrolytic Kinetic Studies." *Bioresource Technology* 236 (7): 155–63.

Mallick, D., M. K. Poddar, P. Mahanta, and V. S. Moholkar. 2018. "Discernment of Synergism in Pyrolysis of Biomass Blends Using Thermogravimetric Analysis." *Bioresource Technology* 261: 294–305.

Mohd Din, A. T., B. H. Hameed, and A. L. Ahmad. 2005. "Pyrolysis Kinetics of Oil-Palm Solid Waste." *Engineering Journal of the University of Qatar* 18 (7): 57–66.

Müsellim, E., M. H. Tahir, M. S. Ahmad, and S. Ceylan. 2018. "Thermokinetic and TG/DSC-FTIR Study of Pea Waste Biomass Pyrolysis." *Applied Thermal Engineering* 137: 54–61.

Onochie, U. P., H. J. Itoje, N. Itabor, P. Akhator, and G. Ojarafe. 2015. "Calorific Value of Palm Oil Residues for Energy Utilisation." *International Journal of Engineering Innovation & Research* 4 (4): 664–7.

Özsin, G., and A. E. Pütün. 2019. "TGA/MS/FT-IR Study for Kinetic Evaluation and Evolved Gas Analysis of a Biomass/PVC Co-pyrolysis Process." *Energy Conversion and Management* 182: 143–53.

Pianroj, Y., S. Jumrat, W. Werapun, S. Karrila, and C. Tongurai. 2016. "Scaled-Up Reactor for Microwave Induced Pyrolysis of Oil Palm Shell." *Chemical Engineering and Processing: Process Intensification* 106 (8): 42–9.

Rasool, T., and S. Kumar. 2020. "Kinetic and Thermodynamic Evaluation of Pyrolysis of Plant Biomass Using TGA." *Materials Today: Proceedings* 21: 2087–95.

Reddy, B. R., B. Shravani, B. Das, P. S. Dash, and R. Vinu. 2019. "Microwave-assisted and Analytical Pyrolysis of Coking and Non-coking Coals: Comparison of Tar and Char Compositions." *Journal of Analytical and Applied Pyrolysis* 142 (9): 104614.

Rodilla, I., M. L. Contreras, and A. Bahillo. 2018. "Thermogravimetric and Mass Spectrometric (TG-MS) Analysis of Sub-bituminous Coal-Energy Crops Blends in N_2, Air and CO_2/O_2 Atmospheres." *Fuel* 215 (3): 506–14.

Salema, A. A., R. M. W. Ting, and Y. K. Shang. 2019. "Pyrolysis of Blend (Oil Palm Biomass and Sawdust) Biomass Using TG-MS." *Bioresource Technology* 274 (2): 439–46.

Sata, V., C. Jaturapitakkul, and K. Kiattikomol. 2007. "Influence of Pozzolan from Various By-Product Materials on Mechanical Properties of High-Strength Concrete." *Construction and Building Materials* 21 (7): 1589–98.

Tangchirapat, W., T. Saeting, C. Jaturapitakkul, K. Kiattikomol, and A. Siripanichgorn. 2007. "Use of Waste Ash from Palm Oil Industry in Concrete." *Waste Management* 27 (1): 81–8.

Wang, L., H. Lei, J. Liu, and Q. Bu. 2018. "Thermo Decomposition Behavior and Kinetics for Pyrolysis and Catalytic Pyrolysis of Douglas Fir." *RSC Advances* 8 (1): 2196–202.

White, J. E., W. J. Catallo, and B. L. Legendre. 2011. "Biomass Pyrolysis Kinetics: A Comparative Critical Review with Relevant Agricultural Residue Case Studies." *Journal of Analytical and Applied Pyrolysis* 91 (1): 1–33.

Williams, P. T., and N. Nugranad. 2000. "Comparison of Products from the Pyrolysis and Catalytic Pyrolysis of Rice Husks." *Energy* 25 (6): 493–513.

Yerrayya, A., D. V. Suriapparao, U. Natarajan, and R. Vinu. 2018. "Selective Production of Phenols from Lignin Via Microwave Pyrolysis Using Different Carbonaceous Susceptors." *Bioresource Technology* 270 (12): 519–28.

Yin, C. Y., S. A. S. A. Kadir, Y. P. Lim, S. N. Syed-Ariffin, and Z. Zamzuri. 2008. "An Investigation into Physicochemical Characteristics of Ash Produced from Combustion of Oil Palm Biomass Waste in a Boiler." *Fuel Processing Technology* 89 (7): 693–6.

Zhang, Y., P. Chen, S. Liu, P. Peng, M. Min, Y. Cheng, E. Anderson, N. Zhou, L. Fan, C. Liu, and G. Chen. 2017. "Effects of Feedstock Characteristics on Microwave-Assisted Pyrolysis – A Review." *Bioresource Technology* 230 (4): 143–51.